Seismic performance of tank models with most unfavourable initial geometric defects imposed under El-centro seismic waves

Ying Sun[a], Yansong Bi*

Northeast Petroleum University, Daqing 163318, China

[a]17860639955@163.com
*876850822@qq.com

ABSTRACT. The safety of tanks, as an important device for storing crude oil, is particularly important. Tank is a typical thin-walled cylindrical shell structure, considering that it will inevitably appear in the project a variety of initial geometric defects, which in turn affects the structural mechanical properties of the tank. In this paper, the finite element analysis software ANSYS is used to establish a reasonable finite element analysis model of the tank based on the coupled fluid-solid model, set up EI-Centro waves, through the improved consistent defects modal analysis method, and carry out the seismic time history analysis to analyse the effect of the most unfavourable initial geometrical defects on the structural dynamic response of the tank. The results show that the buckling critical stress of the tank wall under the influence of the most unfavourable initial geometric defect is much larger than the value specified in the code. Under seismic action, the peak acceleration and the peak equivalent stress at each point of the tank wall decrease significantly with the increase of the height of the tank wall.

KEYWORDS: thin-walled cylindrical shell, initial geometric defects, fluid-solid model, time history analysis

1 INSTRUCTIONS

The medium stored in the tank is usually flammable and explosive, especially under the effect of earthquake, the safety performance of the tank is particularly important. Tank structure of the shell radius and thickness of the ratio is usually greater than 1000, is a typical thin shell structure, and the thin shell structure is a defect-sensitive structure, in the actual processing, use, transport and other processes in the project is prone to local convexity, axial offset, out of roundness and other phenomena, such phenomena are referred to as the structure of the initial geometric defects. Such defects are unavoidable and not easy to measure, especially under seismic loading, it is easy to "elephant foot" buckling, rhombic buckling and other destructive phenomena, which in turn has a great impact on the safety performance of the tank.

© The Author(s) 2023
Z. Ahmad et al. (eds.), *Proceedings of the 2023 5th International Conference on Structural Seismic and Civil Engineering Research (ICSSCER 2023)*, Atlantis Highlights in Engineering 24,
https://doi.org/10.2991/978-94-6463-312-2_30

As early as in the 1840s, the effect of defects on the buckling of cylindrical shells began to be considered in engineering design, but the method used is often the introduction of an experimentally obtained reduction factor to solve the problem of the deviation of the actual value from the theoretical value, which is often used in small models and may not be applicable to the actual engineering of large-diameter cylindrical shell.[6,7] carried out an analytical study; abroad for the "elephant foot" deformation of the causes generally hold two views,[9] that the tank wall elephant foot deformation is mainly due to the horizontal movement of the ground driven by the movement of the tank bottom caused by the .[1] that "elephant foot" is caused by the vertical to the ground. [4] investigated the causes of damage to an 8 m diameter and 10 m high liquid storage tank that overturned in 2009 and concluded that corrosion-induced geometrical defects in the tank and the circumferential stresses generated by the liquid inside the tank were the root causes of the tank damage. [10] analytically obtained the "most unfavourable" shape of the initial geometrical defect profile of a cylindrical shell plate by minimizing the load at the limit point. [2] simulated the tank-liquid coupling by using the equivalent mass method through the connection of rigid rods to the unit nodes of the tank, and concluded that the tank-liquid coupling was the cause of the damage. The coupling between the tank and the fluid is simulated by connecting the rigid rods to the unit nodes of the tank to summarise the elastic buckling characteristics of the tank under seismic excitation. In recent years, some scholars have discussed the effects of factors such as the type of seismic wave in the tank and the presence or absence of a floating roof on the liquid storage shaking, wall hydraulics, and wall strains using round low-density polyethylene tanks [5] with a height-to-diameter ratio of 2 as the subject of their studies. The effect of flexible baffles in tanks on the attenuation of stored liquid shaking under different seismic wave types is also discussed using round tanks with height-to-diameter ratios of 3 and 0.75 [8] as well as small square tanks [3].

2 Finite element modelling and validation of storage tanks

2.1 Finite element modelling of storage tanks

In this paper, based on the storage tank model after flow-solid coupling, the most unfavourable initial geometrical defects are imposed and seismic time-range analysis is carried out using the improved consistent defect modal method. Through the ANSYS finite element software to establish the height of 21.68m, filling the bottom diameter of 96m, the maximum liquid depth of 20.18m, the maximum liquid storage capacity of 150,000 cubic metres of vertical steel anchored non-floating roof storage tank model. Tank wall selection of variable wall thickness design processing, wall thickness parameters shown in Table 1, tank steel and liquid storage material parameters shown in Table 2.

Table 1. Tank wall thickness parameter

	Number of laps	Height/mm	Wall thickness/mm	Level depth/mm
Tank wall	1	2980	40	20180
	2	2680	33	17200

plate	3	2680	26	14520
	4	2680	22	11840
	5	2680	17	9160
	6	2680	12	6480
	7	2660	12	3800
	8	2660	12	1140
Base Plate Edge Plate			23	
Base plate Centre Panel			11	

Table 2. Material parameter

Material	Elastic Modulus (N/m²)	Poisson Ratio	Density (kg/m³)	Yield Strength (N/m²)
Mild Steel	2.1×10^{11}	0.3	7850	3.58×10^{8}
Crude	2.0×10^{9}	-	880	

2.2 Validation of finite element models for storage tanks

The reasonableness of the finite element model establishment is verified by calculating the basic cycle vibration formula of the fluid-solid coupling vibration of the storage tank and the storage liquid in the Design Code for Vertical Cylindrical Steel Welded Oil Tanks (GB50341-2014). The formula is shown in (1):

$$T_c = K_c H_w \sqrt{\frac{R}{\delta_3}} \quad (1)$$

Where T_c=Tank fluid-solid coupled vibration cycles（s）; R=Radius of tank bottom (m); δ_3=Thickness at 1/3 height of tank wall (m); H_w=Tank design level (m); K_c=Vibration Periodicity Coefficient for Fluid-Solid Coupling;

According to (1), the intrinsic period of fluid-solid coupling of the storage tank is calculated as 0.5679s, and the intrinsic frequency is calculated as 1.7609 Hz. The result of numerical simulation is 1.7046 Hz, and the error is about 3.2%, which shows that the result of finite element calculation is more reliable and the model is reasonable.

3 Imposition of initial geometric defects

3.1 Code Provisions for Failure of Tank Wall Instability

When the compressive stress value of a storage tank under uniform axial loading reaches the value of the critical stress for buckling, the shell structure will exhibit regular corrugations in the cross-section and buckling damage will occur. The critical buckling stress of the cylindrical shell structure is based on the elastic small deflection theory equation (2):

$$\sigma_{cr} = \frac{1}{\sqrt{3(1-\mu^2)}} \frac{Et}{R} \quad (2)$$

Where μ= Poisson's ratio, E= the modulus of elasticity of the material, t= the weighted thickness of the tank wall, R= the radius of the tank, and substituting into the calculation gives = 58.3 MPa.

3.2 Imposition of the least favourable initial geometric defect

In this paper, the improved consistent defect modal method is used in the introduction of initial geometric defects, and different initial geometric defect distributions of the tank structure are simulated by extracting the first thirty orders of the flexural modes of the tank, then the nonlinear analysis of the structural stability is carried out by the arc-length method to get the ultimate load carrying capacity of the tanks under the distribution of the different initial geometric defects, and the deformation value of the flexural modes with the lowest load carrying capacity is applied to the perfected model, so as to use the updated tank model as the research object, so as to find the most unfavourable defect distribution form of the tank structure and get the tank model with initial geometric defects.

In ANSYS nonlinear analysis, eigenvalue buckling analysis is carried out on the perfect tank structure to extract the first thirty orders of buckling modes and eigenvalues, and the product of the obtained eigenvalues and external load is the critical buckling stress of the structure. Combined with the results of the arc length method, the critical stress of the cylindrical shell in the first thirty orders of buckling is shown in Figure 1. The buckling critical stress of the tank in the 1st order buckling mode is 37.2 MPa, the minimum critical stress for buckling in 16th order buckling mode is 35.6 MPa. Therefore, in this paper, the deformation value of the 16th order buckling mode is selected, and is applied to the perfect model by modifying the model displacement in order to get the most unfavourable form of the initial geometrical defects, and then to consider the effect of the initial geometrical defects on the static and dynamic performances of the tank. The effect of initial geometric defects on the static and dynamic performance of the tank is then considered. The 16th order buckling modes are shown in Figure 2.

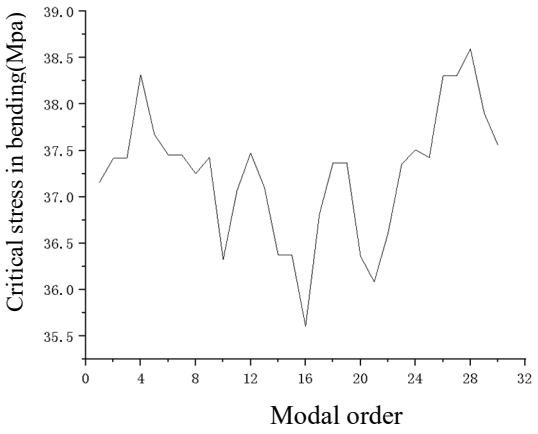

Fig. 1. Analysis results of the first 30 buckling modes by arc length method

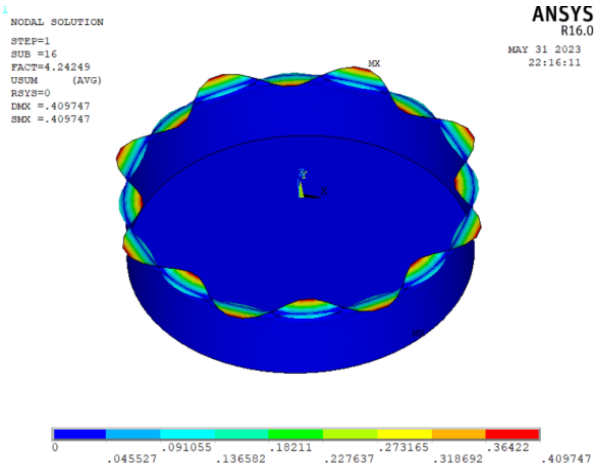

Fig. 2. 16th-order buckling mode

The buckling critical stress of 35.6 MPa is obtained by the improved consistent defect modal method, which is 63.8% less than the theoretical method, indicating that for the tank structure, the improved consistent defect method is more suitable for engineering practice by considering the influence of defects.

4 Seismic Response Analysis of Storage Tanks with Initial Geometrical Defects

4.1 Selection of seismic waves

In the study related to time-range analysis of buildings, two groups of seismic records actually existing in nature and a set of artificially simulated seismic wave data are generally selected to analyse the seismic response of the structure. Combined with the three elements of seismic wave selection, the seismic grouping of tank design in this paper is the second group, the site category is Class II site, the design basic seismic acceleration value is 0.20g, the seismic protection intensity is 8 degrees of protection, and EL-centro seismic wave is selected. The acceleration characteristics of this kind of seismic wave are shown in Table 3 below, and the acceleration time curve is shown in Figure. 3. And comprehensively, the selection method of damping ratio in China's seismic code for oil storage tanks combined with fluid-structure coupling, the damping ratio of the storage tank is selected as 2%.

Table 3. Acceleration characteristics of seismic waves

Earthquake wave	Peak acceleration (cm/s^2)	Peak acceleration occurrence time(s)
El-centro	341.7	2.14

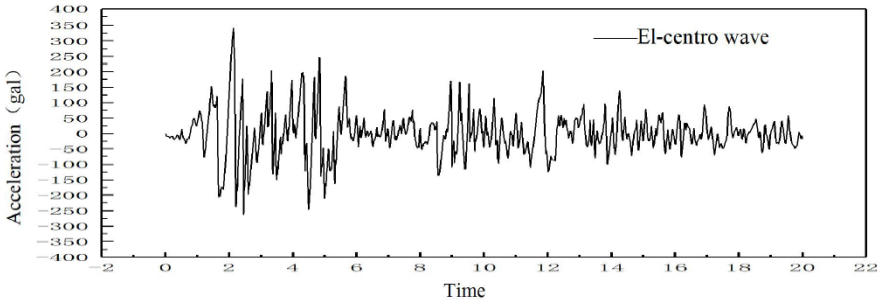

Fig. 3. El-centro wave acceleration time-course curves

4.2 Combination of working conditions and finite element modelling

Two working conditions were selected for comparison: perfect full tank and full tank with defects. Three locations of the tank wall were selected: the bottom 688 nodes at 1m from the tank bottom plate, the middle 1909 nodes at 10m from the tank bottom plate and the top 793 nodes at 19m from the tank bottom plate, as well as the same height of the bottom 603 units, the middle 1980 units and the top 700 units as shown in Figure 4.

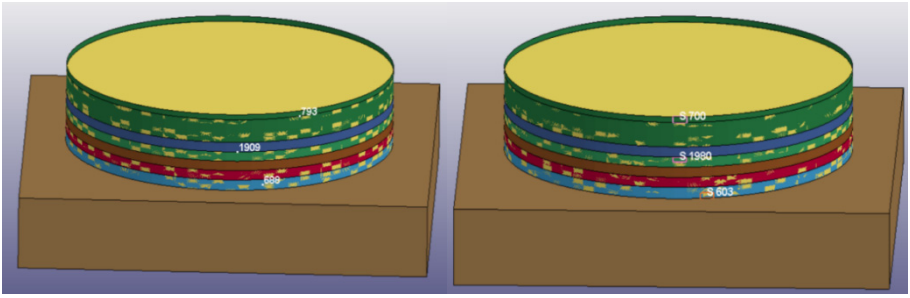

(a)Node location (b)Unit location

Fig. 4. Location of nodes and units selected for storage tank model

4.3 Structural seismic response of storage tanks under El-centro seismic waves

The El-centro seismic wave in X direction was applied to the base of the tank bottom, then the acceleration time-range curves of the top, middle and bottom nodes of the tank wall were extracted as shown in Figure 5 below, and the peak acceleration was extracted from the acceleration time-range curves of the tanks for different working conditions, as shown in Table 4 below.

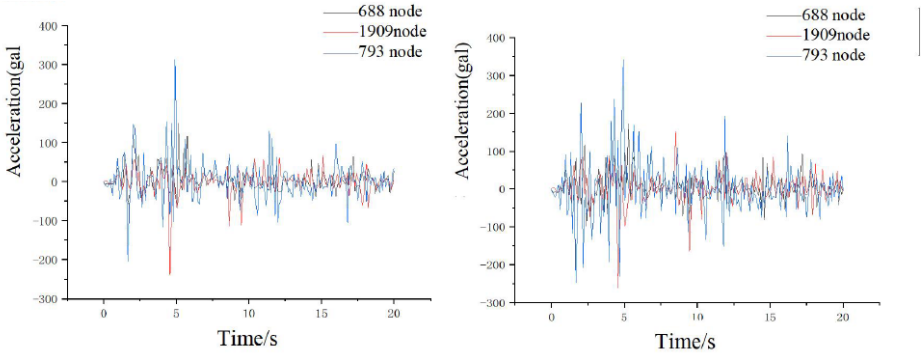

(a)Perfect Full Tank (b)Defective Full Tank

Fig. 5. Time-history curve of node acceleration under El-centro earthquake wave

Table 4. Acceleration peak extraction table under El-centro wave

Location Condition	Perfect peak full tank acceleration (cm/s^2)	Peak defective full tank acceleration (cm/s^2)	Variance Rate (%)
Bottom 688 node	150.2	176.1	14.7
Central 1909 node	237.9	260.8	8.8
Top 793 node	313.2	342.2	8.5

From Figure 5 and Table 4, it can be found that the peak acceleration at the same location of the defective model is greater than that of the perfect model, indicating that the response of the defective tanks to seismic action is more obvious, the greater the

degree of damage, and the worse the seismic capacity. When comparing the peak acceleration at the bottom, middle and top nodes of the tank wall, it is found that the peak acceleration increases with the height of the tank wall. The main reason is that the bottom of the tank wall is connected to the bottom plate, and the bottom plate is connected to the anchorage of the foundation, which has a greater influence on the limitation of acceleration; the middle part of the tank wall is weakly restrained compared to the bottom, and the corresponding peak acceleration is also larger; and the top of the tank is equivalent to the free end, which is not restrained, and it will produce a greater shaking under the excitation of the seismic excitation.

Under the action of El-centro seismic waves, the equivalent force time-range curves of the top, middle and bottom units of the tank wall were extracted as shown in Figure. 6 below, and finally the peak equivalent force was extracted from the acceleration time-range curves for different working conditions, as shown in Table 5 below.

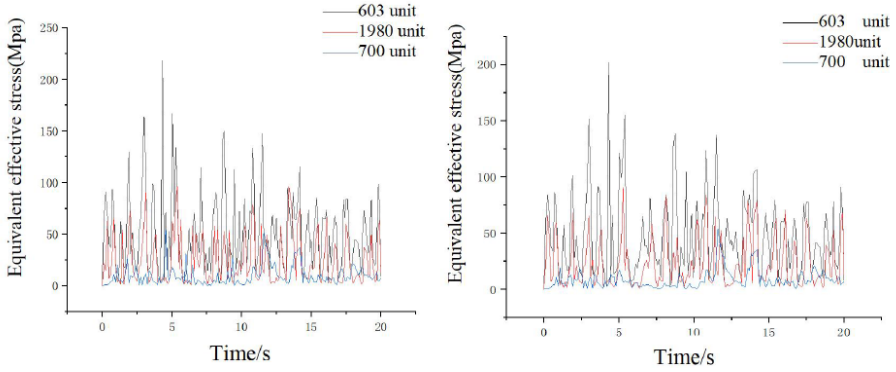

(a)Perfect Full Tank (b)Defective Full Tank

Fig. 6. Time-history curve of equivalent stress of element under El-centro earthquake wave

Table 5. Equivalent stress peak extraction table under El-centro wave

Location Condition	Perfecting the full tank equivalent peak force （MPa）	Peak defective full tank equivalent force （MPa）	Variance Rate （%）
Bottom 603 unit	201.1	224.0	10.2
Central 1980 unit	90.8	98.2	7.5
Top 700 unit	53.8	57.5	6.4

As shown by the time-course curve of equivalent force in Figure 6 and the data in Table 5 Peak Equivalent Force Table, under the effect of earthquake, the wall of the tank is affected by the movement of the liquid in the tank, and the peak equivalent force of the tank wall decreases with the increase of the height of the tank wall. The reason is that the equivalent force of the tank wall gradually increases from top to bottom due to the influence of the liquid inside the tank. The peak equivalent force of the defect-containing model increases to different degrees compared with that of the perfect

model, indicating that the tank wall is affected by the initial geometrical defects, and the equivalent force increases under the seismic excitation, which makes it easy to be damaged and the seismic performance is weakened.

5 Conclusions

In this paper, the finite element software ANSYS is used to establish the tank model, and the validity of the model is verified by comparing the fluid-structure coupling frequency obtained from the modal analysis with the relevant specifications, and then the most unfavourable initial geometric defects are applied to the perfect tank structure by using the improved consistent defects modal method to analyse the seismic response of the tanks under the seismic waves of the El-centro species, and the acceleration and equivalent force of the tanks are analysed and compared with those of perfect tanks and tanks containing the initial geometric defects. Compare the acceleration and equivalent force of the perfect tank with that of the tank with initial geometry defects. Comparing the various methods of calculating the effect of initial geometric defects on the buckling critical stress of the tank wall structure, it is found that for this kind of thin-walled cylindrical shell structure of the tank, the most unfavourable effect of initial geometric defects derived from the improved consistent defects modal method, the buckling critical stress of the tank wall is the smallest but 1.43 times of the result stipulated in the "Code for the Design of Vertical Cylindrical Steel Welded Tanks" (GB50341-2014), from the structural failure of the tank, it is 1.43 times of the result. from the point of view of structural instability considerations, the code provisions are too conservative, the research in this paper can provide a reference for the design optimisation of the code for the value of the buckling critical stress of the storage tank structure.

Under the action of the same seismic wave, the peak acceleration and equivalent force of the bottom of the tank is larger than that of the middle and the upper part, and the corresponding increase in the peak value is also larger, which indicates that the initial geometric defects on the bottom of the tank reduces the magnitude of the seismic performance, which is the reason that the bottom of the tanks containing initial geometric defects is easy to damage under the action of the earthquake, therefore, the bottom of the wall should be taken to take reinforcing measures in the design and construction of the wall, such as setting up reinforcing plates, reinforcing rings and so on. Therefore, reinforcement measures should be taken at the bottom of the tank wall during design and construction, such as setting reinforcement plates, reinforcement rings, etc.

Acknowledgment

Natural Science Foundation of Heilongjiang Province of China (LH2020E018)

REFERENCES

1. AGHAJARI S. ABEDI K. SHOWKATI H. Buckling and post-buckling behavior of Thin-Walled Structures, 2006, 44(8):904-909.
2. Buratt N., Tavan M.. Dynamic buckling and seismic fragility of anchored steeltanks by the added mass method[J]. Earthquake engineering & structure dynamics,2014, 243:1-21.
3. Dinçer A E. Investigation of the sloshing behavior due to seismic excitations considering two-way coupling of the fluid and the structure[J]. Water, 2019, 11(12): 2664.
4. Geary W, Hobbs J. Catastrophic failure of a carbon steel storage tank due to internal corrosion[J]. Case Studies in Engineering Failure Analysis, 2013,1:257-264.
5. Hernandez-Hernandez D, Larkin T, Chouw N, et al. Experimental findings of the suppression of rotary sloshing on the dynamic response of a liquid storage tank[J]. Journal of Fluids and Structures, 2020, 96: 103007.
6. Hornung U, Seal H. Stresses in unanchored tank shells due to settlement of the tank foundation[A]. Proceedings, International Conference on Carrying Capacity of Steel Shell Structures[C], Brno, Czech Republic, 1997:157-163.
7. Palmer SC. Stresses in storage tanks tanks caused by differential settlement[J]. Proceedings of the Institution of Mechanical Engineers, Part E, Journal of Process Mechanical Engineering. 1994,208(EI):5-16.
8. Shekari M R. On the numerical assessment of the resonant sloshing responses in 3D multi baffled partially liquid-filled steel cylindrical tanks shaken by long-period ground motions[J]. Soil Dynamics and Earthquake Engineering, 2020, 129: 105712.
9. SLONE A K. PERICLEOUS K. BAILEY C. Dynamic fluid-structure interaction using finite volume unstructured mesh procedures[J]. Computers and Structures,2002, 80(5):371-390.
10. Tanish D, Ramachandra L S. Computation of worst geometric imperfection profiles of composite cylindrical shell panels by minimizing the non-linear buckling load[J]. Applied Mathematical Modelling, 2019,74.

Open Access This chapter is licensed under the terms of the Creative Commons Attribution-NonCommercial 4.0 International License (http://creativecommons.org/licenses/by-nc/4.0/), which permits any noncommercial use, sharing, adaptation, distribution and reproduction in any medium or format, as long as you give appropriate credit to the original author(s) and the source, provide a link to the Creative Commons license and indicate if changes were made.

The images or other third party material in this chapter are included in the chapter's Creative Commons license, unless indicated otherwise in a credit line to the material. If material is not included in the chapter's Creative Commons license and your intended use is not permitted by statutory regulation or exceeds the permitted use, you will need to obtain permission directly from the copyright holder.